Available online at www.sciencedirect.com

ScienceDirect

Biomedical Journal

journal homepage: www.elsevier.com/locate/bj

Original Article

Physiological and pathophysiological evaluation of baroreflex functionality with concurrent diffusion tensor imaging of its neural circuit in the rat

Ching-Yi Tsai [a], *Jacqueline C.C. Wu* [a], *Shu-Mi Chen* [b,c], *Hsun-Hsun Lin* [d], *Julie Y.H. Chan* [a], *Samuel H.H. Chan* [a,*]

[a] *Institute for Translational Research in Biomedicine, Kaohsiung Chang Gung Memorial Hospital, Kaohsiung, Taiwan*
[b] *Master and PhD Program in Pharmacology and Toxicology, School of Medicine, Tzu Chi University, Hualien, Taiwan*
[c] *Department of Pharmacy, Lotung Poh-Ai Hospital, Yilan, Taiwan*
[d] *Department of Physiology, School of Medicine, Tzu Chi University, Hualien, Taiwan*

ARTICLE INFO

Article history:
Received 3 July 2019
Accepted 21 October 2019
Available online 24 December 2019

Keywords:
Baroreflex functionality
Diffusion tensor imaging
Brain stem
Neural circuit

ABSTRACT

Background: By measuring the prevalence of neuronal traffic between two brain structures based on the notion that diffusion of water molecules along the axon in parallel bundles will create prominent anisotropy in the direction of the passage of action potentials, diffusion tensor imaging (DTI) may be taken as an effective tool for functional investigations. Demonstration of complementary results obtained from synchronized DTI of the baroreflex neural circuit and physiological or pathophysiological evaluation of baroreflex functionality should validate this notion.

Methods: We implemented concurrent changes in neuronal traffic within the neural circuit of the baroreflex-mediated sympathetic vasomotor tone in the brain stem and alterations of its experimental surrogate under physiological and pathophysiological conditions. We further evaluated the functional and clinical implications of results obtained from this experimental paradigm in conjunction with baroreflex induction and a mevinphos intoxication model of brain stem death.

Results: We found that robust connectivity existed between the nucleus tractus solitarii and rostral ventrolateral medulla, the afferent and efferent nuclei of the baroreflex-mediated sympathetic vasomotor. Intriguingly, this connectivity was either reversibly disrupted or irreversibly severed to reflect alterations in baroreflex responses to physiological or pathophysiological challenges.

Conclusions: The capability to observe simultaneous and complementary changes in neuronal traffic within the neural circuit of the baroreflex-mediated sympathetic vasomotor tone and alterations of its experimental surrogate that bears technical, scientific and

* *Corresponding author*. Institute for Translational Research in Biomedicine, Kaohsiung Chang Gung Memorial Hospital, 123, Dapi Rd., Niaosong 833, Kaohsiung, Taiwan.
E-mail address: shhchan@adm.cgmh.org.tw (S.H.H. Chan).
Peer review under responsibility of Chang Gung University.
https://doi.org/10.1016/j.bj.2019.10.006

clinical implications sustains the notion that coupled with relevant physiological phenotypes, DTI can be an effective investigative tool for functional evaluations of brain stem activities.

At a glance of commentary

Scientific background on the subject

By measuring the prevalence of neuronal traffic between two brain structures based on the notion that diffusion of water molecules along the axon in parallel bundles will create prominent anisotropy in the direction of the passage of action potentials, diffusion tensor imaging is an effective tool for functional investigations.

What this study adds to the field

Demonstration of simultaneous and complementary changes in neuronal traffic within the baroreflex neural circuit and physiological or pathophysiological evaluation of baroreflex functionality sustains the notion that coupled with relevant physiological phenotypes; diffusion tensor imaging can be an effective investigative tool for functional assessment of brain stem activities.

Based on physiological (stimulation and lesion), anatomical (tracers), pharmacological (agonists and antagonists) approaches [1,2] and Fos expression [3,4], the neural circuit in the brain stem for baroreflex-mediated sympathetic vasomotor tone has been well established. The key substrates in this neural circuit include the nucleus tractus solitarii (NTS) where primary baroreceptor afferents terminate, the caudal and rostral ventrolateral medulla (CVLM and RVLM), and the sympathetic preganglionic neurons in the thoracic spinal cord. Myriad of publications on normal and abnormal baroreflex functionality has appeared over the last few decades under the assumption that neuronal traffic, or the lack of it, within this neural circuit underpins the execution of short-term and long-term baroreflex regulation of blood pressure (BP). Nevertheless, until recently (see Ref. [5] for review), whether neuronal traffic in the above-mentioned circuit actually takes place in the brain stem during the execution of baroreflex has never been visualized.

Using diffusion of water molecules as the probe to offer information on diffusion anisotropy, diffusion tensor imaging (DTI) has been widely used in studies on normal and abnormal functions of forebrain structures [6–8]. Unlike the forebrain, application of DTI to the brain stem, which requires extraordinary efforts to fine tune the scanning parameters and enhance signal detection, is relatively wanting. Based on successful execution of tractographic analysis of the medulla oblongata in mice [9–12] and rats [13], it has been reported that by measuring the prevalence of traffic within the baroreflex neural circuits based on diffusion anisotropy created in the direction of the passage of action potentials, DTI can be an effective investigative tool for functional evaluations of baroreflex activities when coupled with measurement of relevant cardiovascular phenotypes. Since all the hitherto reports were based on temporal correlation of imaging and physiological results obtained independently but under comparable experimental conditions, implementation of concurrent DTI of the baroreflex neural circuit and evaluation of baroreflex functionality will obviously render confidence that in addition to morphological or pathological evaluations, tractographic analysis can be an effective investigative tool for functional evaluations of brain stem activities.

The goals of this study are two-folded. Our first goal was to implement concurrent tractographic analysis of the baroreflex neural circuit and evaluation of baroreflex functionality in the rat that exhibits stability, versatility and fidelity. Our second goal was to evaluate the physiological and pathophysiological implications of results obtained from simultaneous changes of DTI events in the brain stem and baroreflex-mediated sympathetic vasomotor tone in conjunction with baroreflex induction and a mevinphos intoxication model of brain stem death.

Materials and methods

Ethics statement

All the experimental procedures engaged in this study were approved by the Institutional Animal Care and Use Committee of Kaohsiung Chang Gung Memorial Hospital (IACUC approval number: 2015110502), and were in compliance with the guidelines for animal care and use set forth by that committee. All efforts were made to minimize animal suffering during the experiment and reduce the number of animals used.

Animals

Male adult Sprague–Dawley rats (287–336 g, n = 44) purchased from BioLASCO or the Experimental Animal Center of the Ministry of Science and Technology, Taiwan, were used. Animas were housed in an AAALAC International-accredited Center for Laboratory Animals, with maintained room temperature (24 ± 1 °C) and 12-h light–dark cycles. Rats were allowed to acclimatize for at least 7 days after delivery prior to experimental manipulations. Standard laboratory rat chow and tap water were available *ad libitum*. Animals were assigned in random to be included in the baroreflex-induction group, or to receive treatment with saline or mevinphos.

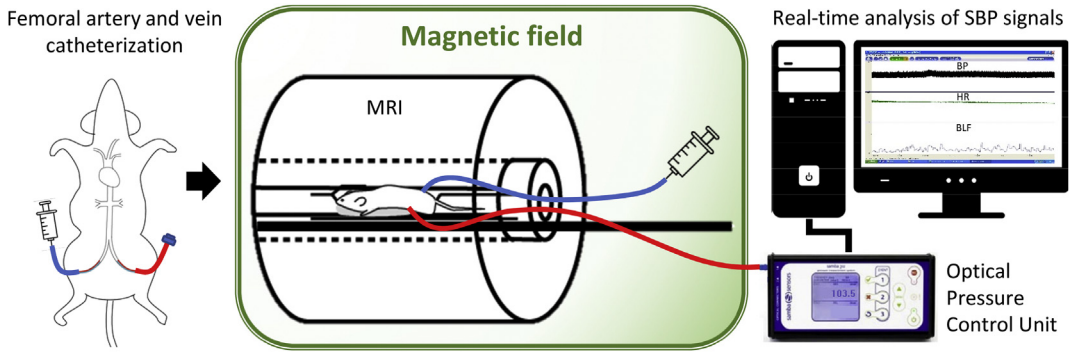

Fig. 1 Experimental setup for synchronized DTI analysis of the baroreflex neural circuit and physiological and pathophysiological evaluations of baroreflex functionality in the rat. Green box represents the magnetic field confines that necessitate using the fiber-optic pressure sensor and fiber glass cable (red line) to connect blood pressure signals detected from the femoral artery to the optical pressure control unit for subsequent real-time spectral analysis of the systolic blood pressure (SBP) signals. Intravenous administration of saline or mevinphos was delivered via a cannulated femoral vein (blue line).

Recording and power spectral analysis of blood pressure signals

Animals received surgery under an initial pentobarbital sodium anesthesia (50 mg kg^{-1}, i.p.) to prepare them for concurrent BP recording, DTI procedures and drug administration [Fig. 1]. Because of the static magnetic field inherent in magnetic resonance imaging (MRI), we paid particular attention to avoid using ferromagnetic materials for catheterization. For this purpose, a fiber-optic miniature pressure measurement system using an ultra-miniature sensor (Samba Preclin 420LP-BIOPAC TSD174A; BIOPAC System, Goleta, CA, USA) was used to cannulate the femoral artery, and a polyethylene tubing (Intramedic PE-20, Clay Adams, Parsippany, NJ, USA) was used for the femoral vein. BP signals recorded from the femoral artery by the sensor were connected to an Optical Pressure Control Unit (Samba 202-BIOPAC MPMS100A-2) placed outside the magnetic field confines [Fig. 1] via a 4-m long fiberglass wire. In some experiments, BP was recorded conventionally by a strain-gauge transducer (BD DTXPlus™, Franklin Lakes, NJ, USA) connected to the femoral artery via a polyethylene tubing (Intramedic PE-50, Clay Adams).

During the recording session, which routinely commenced at least 60 min after pentobarbital induction, animals were anesthetized with 1% isoflurane delivered to the MR bore chamber or via a rat anesthesia mask. In all cases, the recorded BP signals were digitized and processed by an arterial blood pressure analyzer (APR31a, Notocord Systems, Croissy-Sur-Seine, France) based on feature extraction to characterize the BP cycles. Systolic blood pressure (SBP), mean arterial pressure (MAP) and heart rate (HR) were derived from the BP waveforms on a beat-by-beat basis. Continuous, on-line and real-time spectral analysis of SBP signals (SPA10a, Notocord) [14] based on fast Fourier transform was used to detect temporal fluctuations of the low-frequency (BLF) component (0.25–0.8 Hz) in the SBP spectrum. Based on its reduction that mirrors the augmentation of BP [15], and its elimination by sinoaortic denervation [16,17], the power density of the BLF component of the SBP spectrum has been validated to reflect the magnitude of baroreflex-mediated sympathetic vasomotor tone.

Magnetic resonance imaging and diffusion tensor imaging of baroreflex neural circuits in the brain stem

We employed a 9.4T horizontal-bore animal MR scanning system (Biospec 94/20, Bruker, Ettingen, Germany) for sequential MRI/DTI acquisition. This scanning system is made up of a 20-cm clear bore and a gradient insert (BGA-12S; 12-cm inner diameter) that offers a maximal gradient strength of 675 mT m^{-1} and a minimum slew rate of 4673 Tm^{-1} s^{-1}. It is equipped with a rat brain receiver-only coil array using a circular polarized transmitter coil for signal detection from the head. Although the magnet is self-shielded, a room was built around the magnet to create a controlled access area with the borders defined by the 0.5 mT (5 Gauss) contour line of the static magnetic field. During the recording session, animals were anesthetized with 1% isoflurane and the body temperature was maintained at 37 °C by a warm water circulation system.

As a routine, several imaging sequences were executed to evaluate the connectivity between key brain stem neural substrates in the neural circuit of the baroreflex-mediated sympathetic vasomotor tone. High resolution T2-weighted sagittal anatomical reference images were first recorded using multislice turbo rapid acquisition with refocusing echoes sequence to provide the landmark structures for orientation [Fig. 2A]. This was followed by T2-weighted coronal anatomical reference imaging on 11 adjacent slices without gap from a restricted area of the brain stem that covered the medullary portion of the NTS and RVLM or CVLM [Fig. 2B]. Employing identical spatial dimension as in the T2-weighted coronal reference imaging, we evaluated the connectivity between the NTS and RVLM or CVLM, using the spin echo-planar imaging-DTI sequence in the same coronal plane. Imaging the bilateral pyramidal tracts was used as the negative control.

Post-processing of the image data entailed an analysis of fiber tractography between the NTS and CVLM or RVLM on both sides of each animal, using the National Taiwan University DSI studio (http://dsi-studio.labsolver.org). In addition, region-of-interest (ROI)-based analysis was performed [18,19]

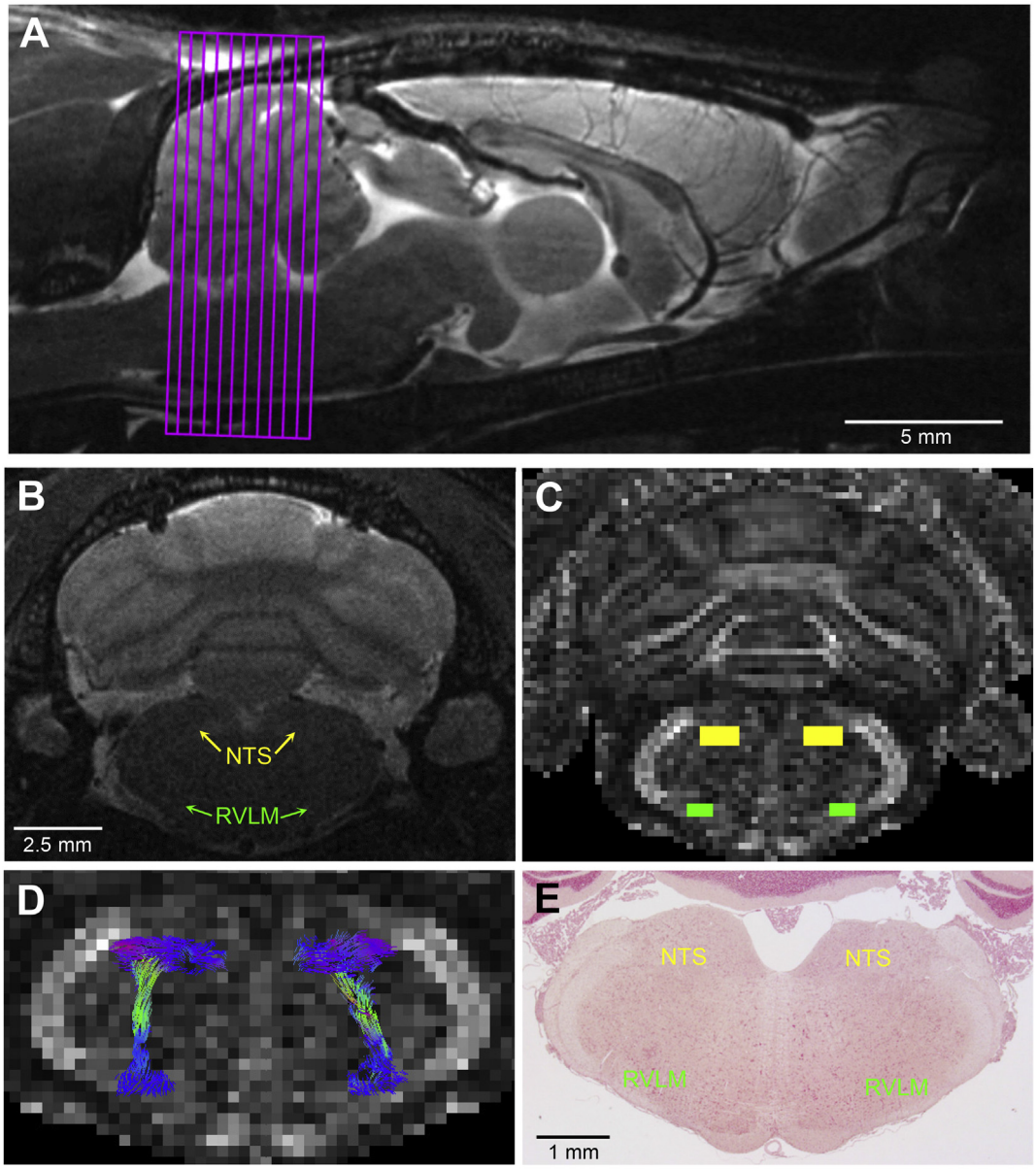

Fig. 2 (A) High resolution T2-weighted sagittal anatomical reference image showing demarcation of the area of the brain stem (rectangular box) that was subjected to tractographic analysis with DTI. (B) T2-weighted coronal anatomical reference image showing detailed locations of the bilateral nucleus tractus solitarii (NTS) and rostral ventrolateral medulla (RVLM). (C) Regions of interest (ROI; yellow or green squares) marked manually on both sides of the fractional anisotropy (FA) map of the brain stem, which correspond to the locations of bilateral NTS and RVLM in the T2-weighted coronal image in (B), to be used to quantify the DTI index, FA. (D) Sample results of tractographic analysis in color-encoded FA map. (E) Photomicrograph of histological section showing location of the NTS and RVLM at the corresponding brain stem level of the FA map in (D).

to quantify a conventional DTI index, fractional anisotropy (FA) [Fig. 2C], which is a scalar value that ranges from 0 (isotropy) to 1 (maximum anisotropy) to describe the degree of anisotropy of a diffusion process, calculated from the eigenvalues ($\lambda 1$, $\lambda 2$, $\lambda 3$). For example, based on the anatomical locations of the NTS and RVLM in the T_2-weighted coronal images [Fig. 2B] and making reference to a rat stereotaxic atlas [20], two ROIs were marked manually on corresponding areas in the FA map on each side of the brain stem [Fig. 2C]. The ROI dimensions for each NTS and RVLM were respectively 3×6 and 2×4 pixels [Fig. 2C]. Starting from the seeds of ROIs, the fiber tracking algorithm proceeded to seek adjacent voxels whose main diffusion direction was in the continuity of the previous one. Representative colors for tractography in color-encoded FA maps [Fig. 2D] were: blue, caudal-rostral; red, left-right; and green, dorsal-ventral. The correct locations of

NTS and RVLM on the FA maps were further verified against histological sections of the brain stem at corresponding levels from the same rat [Fig. 2E].

Induction of baroreflex-mediated sympathetic vasomotor tone

In our physiological evaluation of the baroreflex-mediated sympathetic vasomotor tone, we measured the reflex cardiovascular responses to an increase in BP induced by infusion of norepinephrine (NE; 4 mg kg^{-1} h^{-1}) into the femoral vein for 30 min using a MRI compatible syringe pump (PHD 2000; Harvard Apparatus, Holliston, MA, USA). Temporal alterations in the connectivity between NTS and CVLM or RVLM and the concurrent changes in MAP, power density of the BLF component or HR were measured using a time-window of 30 min.

Mevinphos intoxication model of brain stem death

In our pathophysiological evaluation of the baroreflex-mediated sympathetic vasomotor tone, we employed a mevinphos intoxication model of brain stem death [21]. Mevinphos (Phosdrin; 3-[dimethoxyphosphosphinyl-oxyl]-2-butenoic acid methyl ester) is a US Environmental Protection Agency Toxicity Category I organophosphate. Because of its mode of cardiovascular action, changes in MAP induced by mevinphos are consequential to its actions on the brain stem to elicit an increase followed by a decrease or disappearance of the baroreflex-mediated sympathetic vasomotor tone [14,22]. Since defunct baroreflex-mediated sympathetic vasomotor tone has been demonstrated to be causally related to brain stem death in comatose patients [23–25], the mevinphos intoxication model is suitable for an additional proof-of-principle demonstration of the pathophysiological implication of synchronized DTI of the baroreflex neural circuit and analysis of baroreflex functionality. Temporal alterations in the connectivity between NTS and CVLM or RVLM elicited by intravenous administration of mevinphos (Sigma-Aldrich, St. Louis, MO, USA) at its LD_{50} dose (960 μg kg^{-1}) and the concurrent changes in power density of the BLF component, MAP or HR were measured using a time-window of 30 min. Intravenous injection of the same amount of normal saline served as the vehicle and volume control.

Histology

The brain stem was removed immediately after animals were killed with an over-dose of pentobarbital and fixed in 4% paraformaldehyde. Paraffin-embedded sections (5 μm thickness) were stained by neutral red solution (1%) for 1 min, rinsed with distilled water, dehydrated with ethanol and cleared with xylene for histological verifications.

Statistical analyses

All values are given as mean ± SD. The temporal changes in FA, averaged value of MAP, HR or power density of BLF component in the SBP spectrum calculated every 30 min before or after administration of NE, saline or mevinphos were used for statistical analyses. Two-way analysis of variance with repeated measures was used to assess group means, followed by the Dunnett or Scheffé multiple range test for post hoc assessment of individual means. $p < 0.05$ was considered statistically significant. To better illustrate the spread of data points, group data were additionally presented as group scatter plots.

Results

Visualizing the neural circuit in brain stem for baroreflex-mediated sympathetic vasomotor tone

Because of the size of the medulla oblongata, tractographic analysis of the baroreflex neural circuit demands extraordinary efforts to fine tune the scanning parameters to supplement the enhancement of signal detection by hardware. Tables 1–3 present the results of our systematic optimization of the scanning parameters for T_2-weighted sagittal anatomical reference imaging of the brain [Table 1], coronal anatomical imaging of a restricted brain stem area that contains the medullary portion of NTS, RVLM or CVLM [Table 2],

Table 1 Optimal parameters for T_2-weighted sagittal anatomical reference imaging of the brain of the rat, using multislice turbo rapid acquisition with refocusing echoes (Turbo-RARE) sequence.

Parameter	
Field of view	35 mm × 17.5 mm
Matrix dimension	384 × 192 pixels
Spatial resolution	91 μm × 91 μm
Slice thickness	500 μm
Interslice distance	500 μm
Echo time	14 ms
Effective echo time	42 ms
Repetition time	3000 ms
Rare factor	8
Number of averages	7
Total acquisition time	8 m 24 s

Table 2 Optimal parameters for T_2-weighted coronal anatomical imaging of a restricted area of the brain stem that covered the medullary portion of the nucleus tractus solitarii (NTS) and rostral and caudal ventrolateral medulla (RVLM, CVLM) of the rat, using multislice turbo rapid acquisition with refocusing echoes (Turbo-RARE) sequence on eleven 400-μm slices without gap.

Parameter	
Field of view	20 mm × 20 mm
Matrix dimension	256 × 256 pixels
Spatial resolution	78 μm × 78 μm
Slice thickness	400 μm
Interslice distance	400 μm
Echo time	10 ms
Effective echo time	30 ms
Repetition time	3000 ms
Rare factor	8
Number of averages	8
Total acquisition time	12 m 48s

Table 3 Optimal parameters for diffusion tensor imaging (DTI) between the NTS and RVLM or CVLM of the rat, using spin echo-planar imaging-DTI sequence in the coronal plane covering the same eleven 400-μm slices in the T_2-weighted coronal reference images without gap (Adapted from Ref. [9]).

Parameter	
Field of view	20 mm × 20 mm
Matrix dimension	96 × 96 pixels
Spatial resolution	208 μm × 208 μm
Slice thickness	400 μm
Interslice distance	400 μm
Echo time	19.5 ms
Repetition time	4500 ms
Number of diffusion directions	46
Optimized b value/direction	1500 s/mm^2
Number of b0 images	5
Gradient duration	2.7 ms
Gradient separation	10 ms
Number of averages	4
Acquisition time	30 m 36 s

and imaging the connectivity between these medullary nuclei using spin echo-planar imaging-DTI sequence [Table 3]. Based on those scanning parameters, robust connectivity [Fig. 2D] between histologically verified [Fig. 2E] NTS and RVLM was consistently and amply detected.

We recognize that the contemporary dogma [1,2] stipulates that the CVLM participates in baroreflex-mediated sympathetic vasomotor tone by acting as a synaptic relay that connects the NTS to the RVLM. Functionally, CVLM exerts an inhibitory action on RVLM neurons involved in the tonic and reflex control of sympathetic vasomotor tone. Interestingly, based on 139 scans that we have carried out in rats in this and parallel studies, we rarely (24 out of 278 bilateral evaluations; $p < 0.0001$, Chi-square analysis) detected the obligatory presence of the connectivity between NTS and CVLM in an anterior-posterior presentation of the FA map of the medulla oblongata.

Changes in NTS-RVLM connectivity reflect alterations in functionality of baroreflex-mediated sympathetic vasomotor tone under physiological conditions

Our first set of results ascertained that the changes in connectivity between NTS and RVLM genuinely reflect the physiological functionality of the baroreflex-mediated sympathetic vasomotor tone. As shown in Fig. 3 and quantified in Table 4, an increase in MAP induced by intravenous infusion of NE was accompanied by a temporally correlated decrease in the power density of the BLF component of SBP signals, our experimental index for baroreflex-mediated sympathetic vasomotor tone [15,17] and HR. Concurrent tractographic analysis showed a discernible elevation of the connectivity between NTS and RVLM [Fig. 3] and a significant augmentation of FA [Table 4], the DTI index. Of interest was that the NTS-RVLM connectivity and the power density of the BLF component of SBP signals reversed to pre-infusion levels in a parallel fashion on return of MAP to baseline after termination of NE infusion.

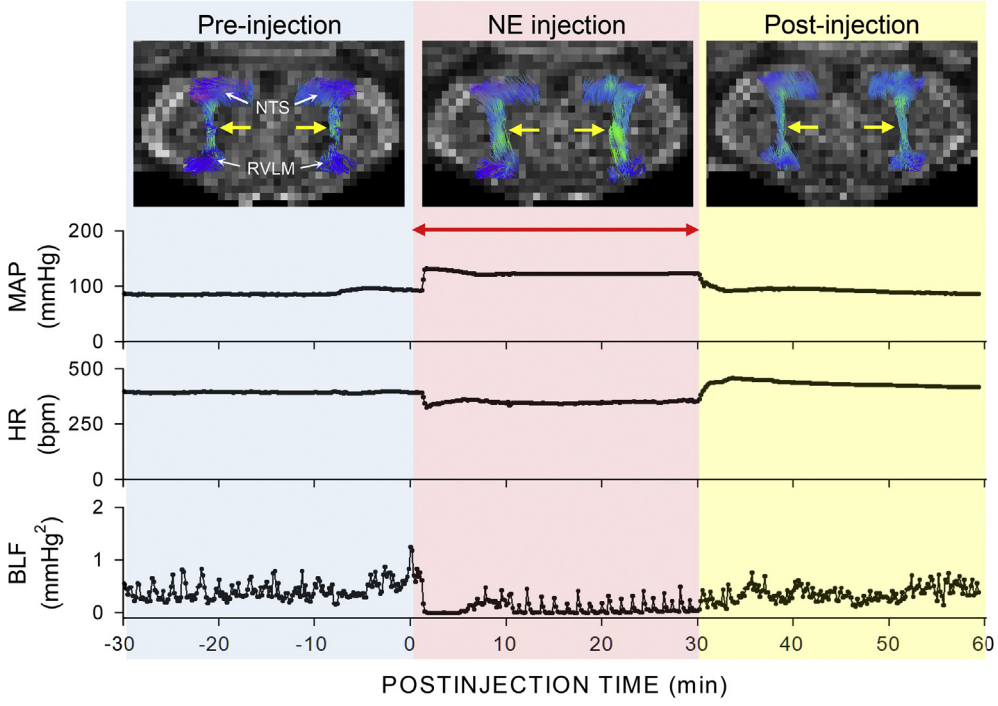

Fig. 3 Representative example of concurrent imaging of connectivity (yellow arrows) between the NTS and RVLM by DTI and measurement of mean arterial pressure (MAP), heart rate (HR) or power density of the low-frequency component (BLF) of SBP spectrum before, during and after 30 min of intravenous infusion (at red arrow) of norepinephrine (NE; 4 mg kg^{-1} h^{-1}) to rats. Note in this and Figs. 4 and 5, representative colors for tractography in color-encoded FA maps are: blue, caudal-rostral; red, left-right; and green, dorsal-ventral.

Table 4 Temporal changes in mean arterial pressure (MAP), heart rate (HR), power density of the low-frequency component (BLF) of SBP spectrum, fractional anisotropy (FA) between the NTS and RVLM or in the pyramidal tracts (PY) in rats that received intravenous administration of norepinephrine (NE; 4 mg kg^{-1} h^{-1}) for 30 min.

	Pre-injection	NE	Post-injection
MAP (mmHg)	96 ± 5	113 ± 7*	94 ± 5
HR (bpm)	366 ± 23	328 ± 20*	368 ± 25
BLF ($mmHg^2$)	0.43 ± 0.15	0.22 ± 0.16*	0.43 ± 0.15
FA (NTS-RVLM)	0.278 ± 0.015	0.307 ± 0.008*	0.276 ± 0.014
FA (PY)	0.326 ± 0.034	0.328 ± 0.019	0.325 ± 0.035

Values are mean ± SD, n = 6 animals. *$p < 0.05$ versus Pre-injection group in the post hoc Dunnett multiple-range analysis.

Our second set of results demonstrates the stability of our experimental paradigm. We observed that superimposed on steady MAP, HR and BLF power 30 min before and 60 min after intravenous administration of saline [Figs. 4 and 6] was the simultaneous exhibition of consistent and stable connectivity between the NTS and RVLM manifested either graphically by the robust dorsal-ventral signals [Fig. 4] or quantitatively by FA [Fig. 6].

Changes in NTS-RVLM connectivity also reflect alterations in functionality of baroreflex-mediated sympathetic vasomotor tone under pathophysiological conditions

Our third set of results demonstrates the versatility of our experimental paradigm by showing that changes in connectivity between NTS and RVLM also reflect alterations in pathophysiological functionality of the baroreflex-mediated sympathetic vasomotor tone. For this part of our study, we took advantage of two fashions of cardiovascular responses to mevinphos at its LD_{50} dose. On intravenous administration at 960 μg kg^{-1}, 50% of the rats underwent a significant increase in our index for baroreflex-mediated sympathetic vasomotor tone and MAP, alongside discernible but insignificant elevation of HR; to be followed by the return of all parameters to the basal level [Figs. 5A and 6]. Concurrent tractographic analysis [Fig. 5A] revealed that the robust NTS-RVLM connectivity before mevinphos administration exhibited an appreciable reduction that was concomitant with the increase in BLF power. Intriguingly, the connectivity between the NTS and RVLM was re-established when the power density of the BLF component of SBP signals returned to basal level. Quantification of the magnitude of NTS-RVLM connectivity by FA yielded comparable results [Fig. 6].

Administration of mevinphos at its LD_{50} dose also resulted in fatality in half of the rats tested. After a very brief increase, there was an abrupt and significant reduction in the power density of the BLF component of SBP signals, MAP and HR, followed by death of the animals [Figs. 5B and 6]. Intriguingly, even within this short duration of 7–8 min after injection of mevinphos, we noted that the index of baroreflex-mediated sympathetic vasomotor tone reached zero [Fig. 5B, blue dashed line] before the exhibition of asystole [Fig. 5B, red dashed line]. Clinically, this signifies brain stem death in comatose patients despite the presence of reasonable SBP and maintained HR [23–25]. Concurrent tractographic analysis of the brain stem again demonstrated that the NTS-RVLM connectivity was severed coincidental

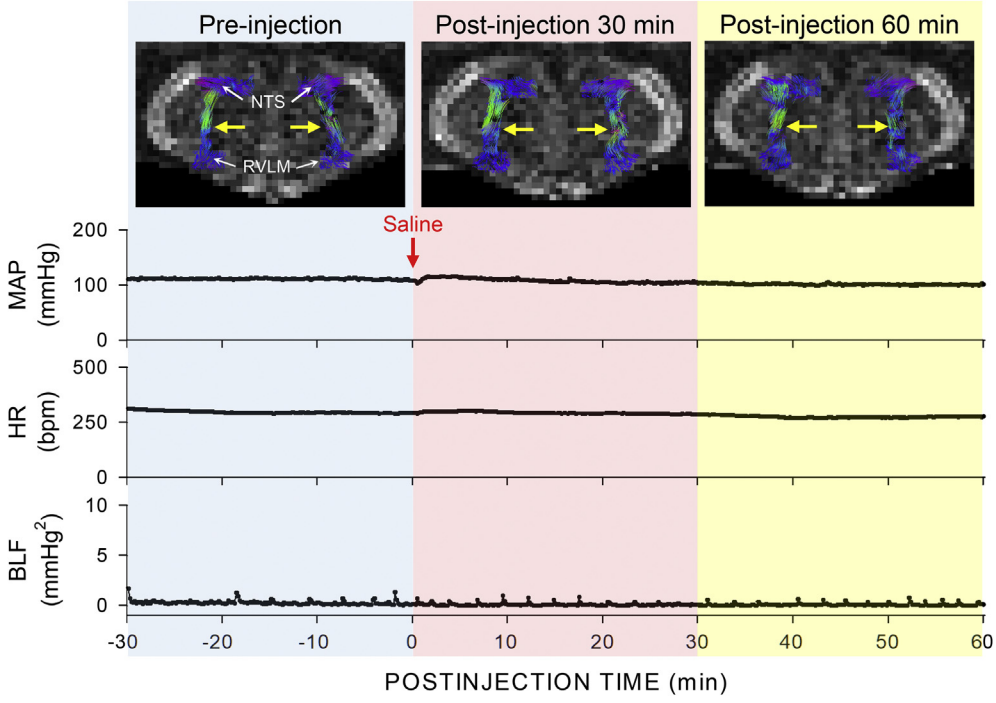

Fig. 4 Representative example of concurrent imaging of connectivity (yellow arrows) between the NTS and RVLM by DTI and measurement of MAP, HR or BLF power 30 min before and 30 or 60 min after intravenous administration of saline (at red arrow) to rats.

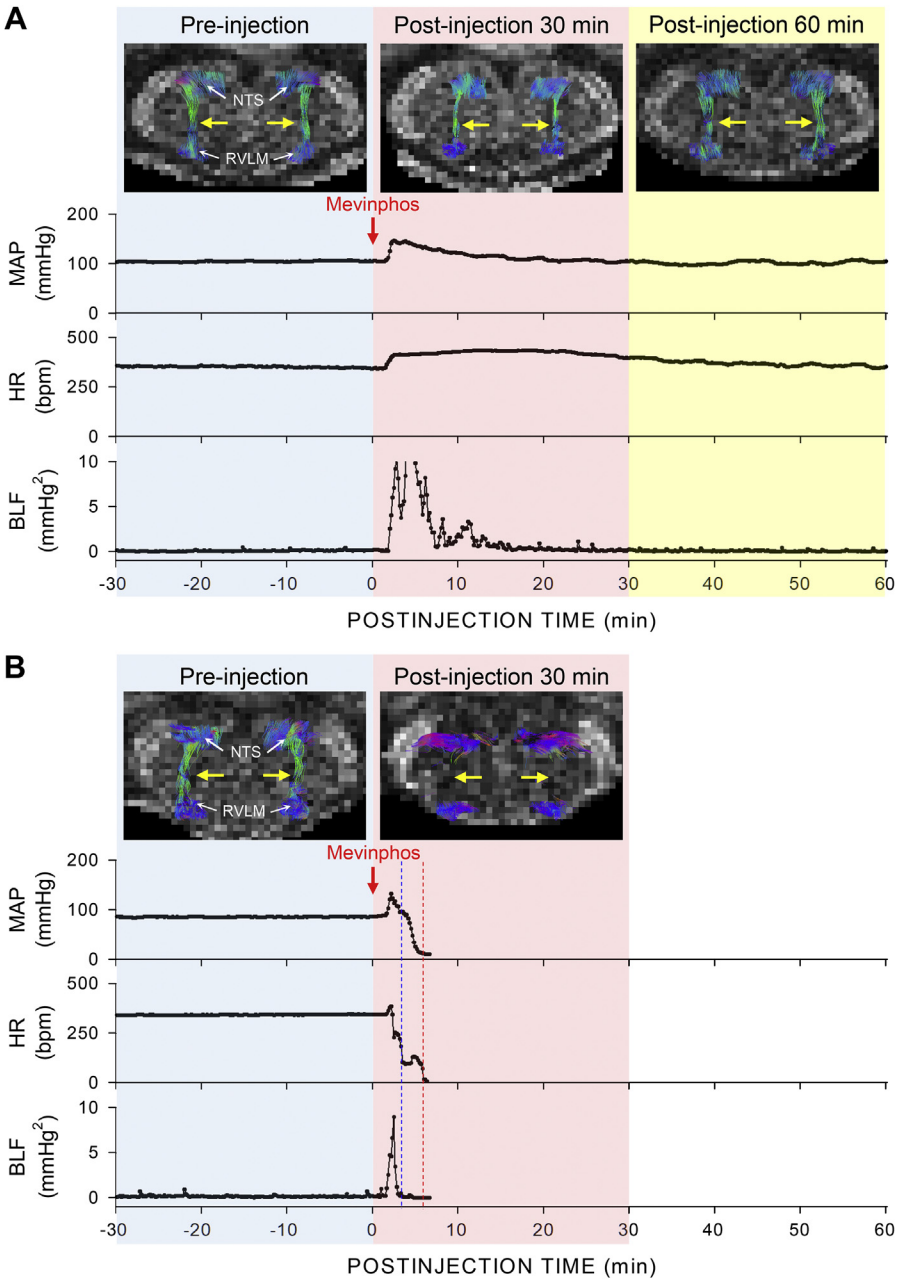

Fig. 5 Representative example of concurrent imaging of connectivity (yellow arrows) between the NTS and RVLM by DTI and measurement of MAP, HR and BLF power 30 min before and 30 or 60 min in rats that survived (A) or died (B) after intravenous administration (at red arrow) of mevinphos (960 μg kg^{-1}). Note the time point when brain death or cardiac death occurs is denoted respectively by blue and red dashed line.

with the loss of baroreflex-mediated sympathetic vasomotor tone [Fig. 5B]. Again, quantification by FA revealed comparable results [Fig. 6].

To further demonstrate the fidelity of our experimental paradigm, we found that the changes in MAP, HR or the power density of the BLF component of SBP signals in response to intravenous administration of mevinphos recorded concurrently with DTI were comparable to those recorded under the same experimental setting but without MR scanning or those obtained under the conventional laboratory setting using polyethylene tubing and strain-gauge transducer [Table 6].

Lack of corresponding DTI changes in pyramidal tract

As a negative control, tractographic analysis of the bilateral pyramidal tracts, which do not play a role in baroreflex-mediated sympathetic vasomotor tone, showed consistent FA values only in the caudal-rostral direction [Tables 4 and 5]

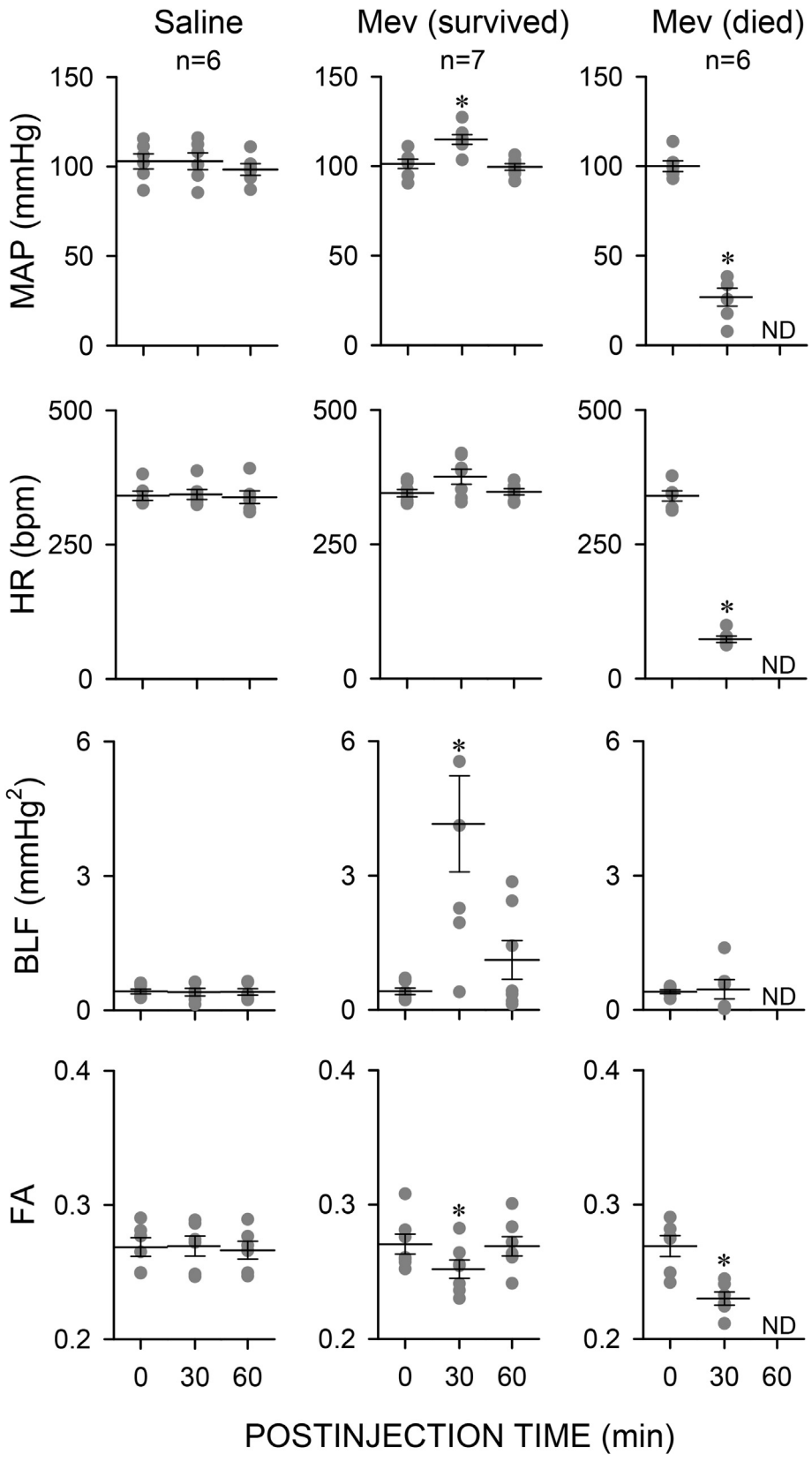

Fig. 6 Temporal changes in MAP, HR, BLF power or FA between the NTS and RVLM in rats that received intravenous administration of saline or survived or died after intravenous administration of mevinphos (960 μg kg^{-1}). Values are mean ± SD, n = 6–7 animals per group. Note that group data from Table 6 are presented as scatter plots to illustrate the spread of data points. *$p < 0.05$ versus Pre-injection control group in the post hoc Dunnett multiple-range analysis, or versus corresponding saline group in the post hoc Scheffé multiple range analysis. Abbreviation: ND: not detected.

Table 5 Temporal changes in fractional anisotropy (FA) in the pyramidal tracts after intravenous administration of saline or mevinphos (Mev; 960 μg kg^{-1}).

	Pre-injection	Post-injection 30 min	Post-injection 60 min
Saline (n = 6)	0.326 ± 0.033	0.329 ± 0.037	0.330 ± 0.036
Mev (survived) (n = 7)	0.334 ± 0.029	0.328 ± 0.028	0.325 ± 0.036
Mev (died) (n = 6)	0.332 ± 0.020	0.336 ± 0.020	ND

Values are mean ± SD, n = 6–7 animals. No significance among all groups ($p > 0.05$) in two-way ANOVA with repeated measures. Abbreviation: ND: not detected.

in animals that received intravenous infusion of NE, administration of saline or animals that survived or died after mevinphos treatment.

Discussion

This article details the implementation of concurrent tractographic analysis of baroreflex neural circuit and evaluation of baroreflex functionality in the rat. Using NTS-RVLM connectivity and baroreflex-mediated sympathetic vasomotor tone as an illustrative example, in conjunction with baroreflex induction and the mevinphos intoxication model of brain stem death, we further demonstrated that this experimental paradigm exhibits stability, versatility and fidelity, and the results obtained bear physiological and pathophysiological implications.

Table 6 Comparison of temporal changes in MAP, HR or BLF power obtained in rats that survived intravenous administration of mevinphos (960 μg kg^{-1}) using miniature fiber-optic pressure sensor and fiberglass connecting cable (FF) and with or without MR scanning; or conventionally with strain-gauge transducer and cannulation of femoral artery with polyethylene tubing (PE).

	Pre-injection	Post-injection 30 min	Post-injection 60 min
MAP (mmHg)			
FF with MRI (n = 7)	101.2 ± 6.8	114.8 ± 7.1*	99.5 ± 4.8
FF without MRI (n = 6)	99.1 ± 4.1	114.5 ± 5.5*	101.0 ± 4.2
PE without MRI (n = 5)	99.6 ± 4.9	112.4 ± 3.8*	100.3 ± 4.5
HR (bpm)			
FF with MRI	345.1 ± 18.4	375.8 ± 37.3*	347.4 ± 15.5
FF without MRI	344.4 ± 15.4	374.2 ± 18.5*	347.5 ± 14.9
PE without MRI	345.5 ± 16.8	370.7 ± 9.1*	348.3 ± 6.0
BLF (mmHg^2)			
FF with MRI	0.41 ± 0.18	4.15 ± 2.84*	1.11 ± 1.13
FF without MRI	0.45 ± 0.18	4.15 ± 1.43*	1.38 ± 0.74
PE without MRI	0.41 ± 0.10	4.07 ± 1.14*	1.53 ± 0.57

Values are mean ± SD, n = 5–7 animals per experimental group. *$p < 0.05$ versus corresponding Pre-injection group in the post hoc Dunnett multiple-range analysis. No statistical significance across the three experimental groups ($p > 0.05$) in two-way ANOVA with repeated measures.

Physiological implications

As pointed out in a recent review [5], DTI uses water molecules as the probe to offer information on diffusion anisotropy, and tractographic analysis investigates brain connectivity. Since the diffusion of water molecules along the axon in parallel bundles will create prominent anisotropy in the direction of the passage of action potentials, it is reasoned that changes in FA can be taken to infer augmentation, reduction or cessation of impulse traffic between two brain structures, which were termed elevation, disruption or severance of functional connectivity. The capability to observe simultaneous changes in neuronal traffic within the neural circuit of the baroreflex-mediated sympathetic vasomotor tone and alterations of its experimental surrogate, the power density of the BLF component of the SBP signals, therefore represents a meaningful advancement in physiological methodology.

The implementation of concurrent tractographic analysis of baroreflex neural circuit and evaluation of baroreflex functionality in the rat bear at least two noteworthy physiological implications. The first implication is that neuronal traffic in the neural circuit in the brain stem indeed takes place during the execution of baroreflex. More intriguingly, the second implication concerns the contemporary neural circuit for baroreflex-mediated sympathetic vasomotor tone, which depicts the CVLM as an intermediate between the NTS and RVLM [1,2]. We rarely detected the obligatory presence of connectivity between NTS and CVLM in an anterior-posterior presentation of the FA map of the medulla oblongata. Nevertheless, commensurate temporal changes in NTS-RVLM connectivity and baroreflex-mediated sympathetic vasomotor tone shown in Figs. 3–5 were consistently demonstrated. In hindsight, our initial attempt to visualize this arm of the baroreflex based on identification of the obligatory NTS-CVLM connectivity has stalled our progress for no less than 9 months. It was only after we resolved that this connection is essentially absent from the neural circuit of baroreflex-mediated sympathetic vasomotor tone that we were able to move forward with the development of our experimental paradigm.

Direct projection of barosensitive NTS neurons to the RVLM has been reported in rabbits [26] and rats [3,27], and the possibility exists for those NTS neurons to synapse with GABAergic interneurons in the RVLM [28]. It is therefore conceivable that, similar to mice [9,12], the baroreflex-mediated sympathetic vasomotor tone in rats is also sustained by a tonic inhibitory input from the NTS to RVLM, which in turn lessens the tonic excitatory action of these premotor sympathetic neurons on vasomotor tone. To offer credence to this notion, we demonstrated that the reflex decrease in sympathetic vasomotor tone in response to elevation of MAP induced by the infusion of NE is concomitant with augmentation in the NTS-RVLM connectivity [Fig. 3] indicative of enhanced inhibition of RVLM neurons from the NTS. We further showed that a reduction in FA between NTS and RVLM indicative of disinhibition of RVLM neurons is

concurrent with an increase in BLF power during the first 30 min in rats that survived mevinphos [Figs. 5A and 6].

We are cognizant that detection of DTI signals is determined by the threshold set by the algorithm that stitches together adjacent voxels. It is therefore certainly true that one can manipulate the appearance and disappearance of DTI signals by adjusting the threshold conditions. Nevertheless, this is not the case in our experimental design because we employed exactly the same scanning parameters and settings for post-processing of the images in all segments of our study. Based on this design, we demonstrated not just disappearance but also decrease and increase in NTS-RVLM connectivity. More importantly and in physiological terms, we consistently showed that those changes in connectivity between the NTS and RVLM were temporally commensurate with corresponding alterations in baroreflex-mediated sympathetic vasomotor tone.

Clinical implications

Our pathophysiological observations also bear clinical implications. Specifically, it allowed us to conclude that whether an animal will survive or die in our mevinphos intoxication model of brain stem death depends on whether the connectivity between the NTS and RVLM is reversibly disrupted (pathophysiology) or is irreversibly severed (pathology). Defunct baroreflex-mediated sympathetic vasomotor tone has been demonstrated to be causally related to brain stem death in comatose patients [23–25]. The presence of an interim when cardiac functions are sustained after brain death until the invariable asystole that follows is one of the driving forces for recognizing brain stem death as the legal definition of death in Taiwan [29], UK [30], US [31] and EU [32]. Fig. 5B amply demonstrates that this sequence of events begins with the cessation of neuronal traffic between the NTS and RVLM, leading to the loss of baroreflex-mediated sympathetic vasomotor tone that signifies brain death, followed by cardiac death.

Technical considerations

The chief hurdle to implement concurrent analysis of the baroreflex neural circuit using DTI and evaluation of baroreflex functionality is the magnetic fields created by the MR scanner, which dictates that no significant magnetically susceptible objects are allowed in the room that houses the magnet. At the same time, the magnetic fields and radiofrequency energy produced by the super-conducting magnet may cause electrically active devices to malfunction, erase magnetic data media, or destroy mechanically-sensitive components. As a result, the physiological monitors for cardiovascular events must be placed outside the confines of the magnetic field. At the same time, it is essential that the sensors, transducers and connecting cables must be on one hand devoid of ferromagnetic materials, and on the other capable to record and transmit BP signals with fidelity. After numerous trials-and-errors, we finally surmounted these difficulties by employing a fiber-optic ultra-miniature sensor to measure BP signals from the femoral artery, and transmitting these signals to an Optical Pressure Control Unit placed outside the confines of the magnetic field via a fiberglass wire. In addition to stability, we demonstrated the fidelity of this recording system by showing that the MAP, HR and baroreflex-mediated sympathetic vasomotor tone determinations were not affected by the magnetic fields during MR scanning, and were comparable to those recorded in a conventional manner based on cannulation of the femoral artery with polyethylene tubing and strain-gauge transducer.

As discussed recently [5,9], in addition to the size, the location of the brain stem in an oblique position from the horizontal plane of the cortical surface and beneath the cerebellum makes its accessibility by MRI difficult. To apply an angled restraining device to the head of the animal to produce an angle between the brain stem/cervical spinal cord and the rest of the body, as suggested for mice [33], is an option. Since we reasoned that this unnatural position would exert extra stress on the rat, we have resorted to placing the cortex in its horizontal position but using a higher magnetic strength (9.4T) to improve signal detection. Together with systematic optimization of the scanning parameters, we were able to obtain high quality T_2-weighted sagittal anatomical reference images of the brain, coronal anatomical images of the medulla oblongata, and DTI images of the connectivity between key components of the baroreflex neural circuits. It should be stressed that, for practical reasons, the scanning parameters in a clinical setting for DTI are by-and-large fixed. On the other hand, for MR scanning in animals, the parameters require fine tuning to obtain optimal results. The scanning parameters reported in Tables 1–3 should therefore be taken as an initial guide for easy implementation of new parameters that befit individual requirements.

Limitations

Despite the technical advancements and the physiological or clinical implications, we recognize that at least two limitations of the reported methods still remain. The first limitation is with the time-window of our evaluations. To obtain optimal results for our DTI analysis, an acquisition time of approximately 30 min was required. By definition, the concomitantly obtained MAP, HR and baroreflex-mediated sympathetic vasomotor tone represent the 30 min average of those cardiovascular responses. We are currently working on shortening this time-window while retaining the quality of our tractographic analysis. Until this goal is realized, the reported method is more suitable for studies that are not designed to measure beat-to-beat cardiovascular events. The second limitation is with the duration of our evaluations. It is obvious that the advantage of synchronized tractographic analysis of baroreflex neural circuits and physiological evaluation of baroreflex functionality will be maximized should the same experimental paradigm be repeated on the same animal over days or perhaps weeks. Unfortunately, the rigidity and fragility of the fiber-optic sensor and the fiberglass connecting cable prevented us from carrying out our experimental paradigm on a repetitive basis. One potential solution is to instrument the rats for radiotelemetric measurements of cardiovascular events. Although MRI-compatible implants for radiotelemetry in rats have been reported [34], its applicability in synchronized DTI analysis and cardiovascular evaluation remains to be established.

Concluding remarks

Using baroreflex-mediated sympathetic vasomotor tone as an example, we report here the implementation of methods that allow for concurrent visualization of neuronal traffic within its neural circuit during the functional execution of baroreflex. In addition to demonstrating its stability, versatility and fidelity, we showed that our experimental paradigm bears physiological and clinical implications. As such, our results substantiate the notion that superimposed on the traditional morphological or pathological evaluations, tractographic analysis offers a hitherto unexplored research dimension as an effective investigative tool for functional evaluations of brain stem activities. On further refinement aiming at resolving its limitations, we envisage that our reported experimental paradigm will open a new vista that allows us to re-examine existing dogmas and create new views on cardiovascular physiology.

Funding

This study was supported in part by the Ministry of Science and Technology, Taiwan [MOST-106-2320-B-182A-014-MY3 for C.Y.T.; MOST-107-2320-B-182A-024 for S.H.H.C.], and the Chang Gung Medical Foundation, Taiwan [CMRPG8E1681, CMRPG8E1682 and CMRPG8E1683 for C.Y.T. and OMRPG8C0021 for S.H.H.C.].

Conflicts of Interest

The authors declare that there are no competing interests.

Acknowledgments

We thank Ms. Chia-Chi Wu for her technical assistance in histological examination.

REFERENCES

[1] Dampney RAL. Functional organization of central pathways regulating the cardiovascular system. Physiol Rev 1994;74:323–64.
[2] Spyer KM. Central nervous mechanisms contributing to cardiovascular control. J Physiol 1994;474:1–19.
[3] Chan RK, Sawchenko PE. Organization and transmitter specificity of medullary neurons activated by sustained hypertension: implications for understanding baroreceptor reflex circuitry. J Neurosci 1998;18:371–87.
[4] Dampney RAL, Horiuchi J. Functional organisation of central cardiovascular pathways: studies using c-fos gene expression. Prog Neurobiol 2003;71:359–84.
[5] Tsai CY, Poon YY, Chan JYH, Chan SHH. Baroreflex functionality in the eye of diffusion tensor imaging. J Physiol 2019;597:41–55.
[6] Horsfield MA, Jones DK. Applications of diffusion-weighted and diffusion tensor MRI to white matter diseases—a review. NMR Biomed 2002;15:570–7.
[7] Lim KO, Helpern JA. Neuropsychiatric applications of DTI—a review. NMR Biomed 2002;15:587–93.
[8] Alexander AL, Lee JE, Lazar M, Field AS. Diffusion tensor imaging of the brain. Neurotherapeutics 2007;4:316–29.
[9] Su CH, Tsai CY, Chang AYW, Chan JYH, Chan SHH. MRI/DTI of the brain stem reveals reversible and irreversible disruption of the baroreflex neural circuits: clinical implications. Theranostics 2016;6:837–48.
[10] Tsai CY, Su CH, Baudrie V, Laude D, Weng JC, Chang AYW, et al. Visualizing oxidative stress-induced depression of cardiac vagal baroreflex by MRI/DTI in a mouse neurogenic hypertension model. Neuroimage 2013;82:190–9.
[11] Tsai CY, Su CH, Leu S, Chang AYW, Chan JYH, Chan SHH. Endogenous vascular endothelial growth factor produces tonic facilitation of cardiac vagal baroreflex via fetal liver kinase-1 in medulla oblongata. Int J Cardiol 2015;187:421–5.
[12] Tsai CY, Poon YY, Chen CH, Chan SHH. Anomalous baroreflex functionality inherent in floxed and Cre-Lox mice: an overlooked physiological phenotype. Am J Physiol Heart Circ Physiol 2017;313:H700–7.
[13] Tsai CY, Su CH, Chan JYH, Chan SHH. Nitrosative stress-induced disruption of baroreflex neural circuits in a rat model of hepatic encephalopathy: a DTI study. Sci Rep 2017;7:40111.
[14] Tsai CY, Chang AYW, Chan JYH, Chan SHH. Activation of PI3K/Akt signaling in rostral ventrolateral medulla impairs brain stem cardiovascular regulation that underpins circulatory depression during mevinphos intoxication. Biochem Pharmacol 2014;88:75–85.
[15] Poon YY, Tsai CY, Cheng CD, Chang AYW, Chan SHH. Endogenous nitric oxide derived from NOS I or II in thoracic spinal cord exerts opposing tonic modulation on sympathetic vasomotor tone via disparate mechanisms in anesthetized rats. Am J Physiol Heart Circ Physiol 2016;311:H555–62.
[16] Cerutti C, Barres C, Paultre C. Baroreflex modulation of blood pressure and heart rate variabilities in rats: assessment by spectral analysis. Am J Physiol Heart Circ Physiol 1994;266:H1993–2000.
[17] Li PL, Chao YM, Chan SHH, Chan JYH. Potentiation of baroreceptor reflex response by heat shock protein 70 in nucleus tractus solitarii confers cardiovascular protection during heatstroke. Circulation 2001;103:2114–9.
[18] Basser PJ, Mattiello J, LeBihan D. MR diffusion tensor spectroscopy and imaging. Biophys J 1994;66:259–67.
[19] Basser PJ, Pierpaoli C. Microstructural and physiological features of tissues elucidated by quantitative-diffusion-tensor MRI. J Magn Reson 2011;213:560–70.
[20] Paxinos G, Watson C. The rat brain in stereotaxic coordinates. 6th ed. New York: Academic Press; 2006.
[21] Chan JYH, Chang AYW, Chan SHH. New insights on brain stem death: from bedside to bench. Prog Neurobiol 2005;77:396–425.
[22] Yen DHT, Yen JC, Len WB, Wang LM, Lee HC, Chan SHH. Spectral changes in systemic arterial pressure signals during acute mevinphos intoxication in the rat. Shock 2001;15:35–41.
[23] Kuo TBJ, Yien HW, Hseu SS, Yang CCH, Lin YY, Lee LC, et al. Diminished vasomotor component of systemic arterial pressure signals and baroreflex in brain death. Am J Physiol 1997;273:H1291–8.
[24] Yien HW, Hseu SS, Lee LC, Kuo TBJ, Lee TY, Chan SHH. Spectral analysis of systemic arterial pressure and heart rate signals as a prognostic tool for the prediction of patient

outcome in intensive care unit. Crit Care Med 1997;25:258–66.
[25] Yen DHT, Yien HW, Wang LM, Lee CH, Chan SHH. Spectral analysis of systemic arterial pressure and heart rate signals of patients with acute respiratory failure induced by severe organophosphate poisoning. Crit Care Med 2000;28:2805–11.
[26] Polson JW, Potts PD, Li YW, Dampney RAL. Fos expression in neurons projecting to the pressor region in the rostral ventrolateral medulla after sustained hypertension in conscious rabbits. Neuroscience 1995;67:107–23.
[27] Ross CA, Ruggiero DA, Reis DJ. Projections from the nucleus tractus solitarii to the rostral ventrolateral medulla. J Comp Neurol 1985;242:511–34.
[28] Meeley MP, Ruggiero DA, Ishitsuka T, Reis DJ. Intrinsic gamma-aminobutyric acid neurons in the nucleus of the solitary tract and the rostral ventrolateral medulla of the rat: an immunocytochemical and biochemical study. Neurosci Lett 1985;58:83–9.
[29] Hung TP, Chen ST. Prognosis of deeply comatose patients on ventilators. J Neurol Neurosurg Psychiatry 1995;58:75–80.
[30] Pallis CA, Prior PF. Guidelines for the determination of death. Neurology 1983;33:251–2.
[31] Wijdicks EFM. Determining brain death in adults. Neurology 1995;45:1003–11.
[32] Haupt WF, Rudolf J. European brain death codes: a comparison of national guidelines. J Neurol 1999;246:432–7.
[33] Kim JH, Song SK. Diffusion tensor imaging of the mouse brain stem and cervical spinal cord. Nat Protoc 2013;8:409–17.
[34] Nölte I, Gorbey S, Boll H, Figueiredo G, Groden C, Lemmer B, et al. Maintained functionality of an implantable radiotelemetric blood pressure and heart rate sensor after magnetic resonance imaging in rats. Physiol Meas 2011;32:1941–51.